Orthogonal, Exactly Periodic Subspace Decomposition

D. Darian Muresan and Thomas W. Parks, *Fellow, IEEE*

***Abstract*—The detection and estimation of machine vibration multiperiodic signals of unknown periods in white Gaussian noise is investigated. New estimates for the subsignals (signals making up the received signal) and their periods are derived using an orthogonal subspace decomposition approach. The concept of exactly periodic signals is introduced. This in turn simplifies and enhances the understanding of periodic signals.**

***Index Terms*—Harmonics, period estimation, periodic signals, signal decomposition, signal transforms.**

I. Introduction

THE ANALYSIS of machine vibrations has proven to be a valuable application of signal processing. A variety of well-known techniques used in this area [1], [2] require that good period and periodic subsignal estimates can be made. Other applications of period estimation techniques are separation of periodic waveforms with overlapping spectra, finding musical rhythms, and generally finding patterns in a wide variety of data sources. The aim here is to develop a method for periodic subsignal estimation.

Related work includes the matrix algebraic separation (MAS) algorithm [3]–[5] for estimating two periodic subsignals and the work of [6]–[8]. In [6], the authors suggest a double difference function (DDF) algorithm, where the composite signal is fed through two cascaded comb filters of the form $h_i(t) = \delta(t) - \delta(t - \tau_i)$. When the lag parameters τ_i correspond to the two periods, the output is everywhere zero. In [7], the authors present a method of detecting subspace signals, in subspace interference, using oblique projections [9]. Applying their idea to the two period estimation problem, one can assume that the first periodic signal is the actual period and that the second periodic signal is the interference. In [8], the authors introduce the concept of periodicity transforms (PTs). The PTs decompose a signal into a sum of periodic sequences by projecting onto sets of periodic subspaces. As the authors note, the results of the PTs depend on the order in which periodic signal components are extracted. The work presented here eliminates this problem by generating orthogonal periodic subspaces.

Manuscript received April 24, 2001; revised February 3, 2003. This work was supported by the Office of Naval Research under Contract N00014-94-1-0102 and the National Science Foundation under Grant MIP9705349. The associate editor coordinating the review of this paper and approving it for publication was Prof. Fredrik Gustafsson.

D. D. Muresan is with Digital Multi-Media Design, Arlington, VA 22209 USA (e-mail: darian@dmmd.net).

T. W. Parks is with Electrical and Computer Engineering, Cornell University, Ithaca, NY 14853 USA (e-mail: parks@ece.cornell.edu).

Digital Object Identifier 10.1109/TSP.2003.815381

In the specific case of dealing with the problem of recovery and detection of multiple sinusoidal signals, there is an entire class of estimators, including periodigram, Prony's Method, Piseranko harmonic decomposition (PHD), MUSIC, ESPRIT, and IQML. (For a review of these methods, see [10, ch. 11] and [11]).

This paper extends the results of [12] to multiple period estimation. It is a more detailed and thorough discussion of the work presented in [13] and [14]. The approach of this paper is to generate orthogonal subspaces that correspond to periods ranging from 1 up to the maximum expected subperiod $(P_{\max})$ of the received signal R. Estimates of the subsignals and their energy are obtained by taking orthogonal projections of R onto these different orthogonal subspaces. This paper begins by analyzing the one- and two-period estimation cases and then generalizes the results to multiple period estimation. Using a vibration signal recorded from a General Motors gear box, the techniques developed here are applied to real vibration data.

This paper is organized as follows. Section II reviews the single period estimation results of [12]. Section III introduces the key concept of *exactly periodic* signals, and Section IV introduces exactly periodic and orthogonal subspaces. Results and implementation discussions are found in Section V. Finally, Section VI concludes with some final thoughts and future work.

II. Single Period Estimation

This section reviews the results of [12] for the single period estimation case. Let $S = \{s_0, \ldots, s_{K_0-1}\}$ be a periodic repetition of the length P sequences $Q = \{q_0, \ldots, q_{P-1}\}$. The received signal $R = \{r_0, \ldots, r_{K_0-1}\}$ of length K_0 (K_0 is a multiple of P) then consists of S plus white, zero mean Gaussian noise $N \sim \mathcal{N}(0, \sigma^2)$

$$R = S + N.$$

For any specific period P, an orthonormal basis set for the subspace of all periodic signals of period P is

$$\{\psi_k\} = \sqrt{\frac{1}{M}}\delta_k$$

where $k = 0, \ldots, P-1, M = K_0/P$, and δ_k is a $K_0 \times 1$ vector with ith entry

$$\delta_k(i) = \begin{cases} 1, & i = k + lP, \quad \text{for integer } l \\ 0, & \text{else.} \end{cases}$$

Let Ψ^P be the orthonormal matrix having $\psi_0, \ldots, \psi_{P-1}$ as column vectors

$$[\Psi^P]_{K_0 \times P} = \sqrt{\frac{1}{M}} \begin{bmatrix} 1 & 0 & \cdots & 0 & 1 & 0 & \cdots & 0 \\ 0 & 1 & \cdots & 0 & 0 & 1 & \cdots & 0 \\ \vdots & \vdots & \vdots & \vdots & \vdots & \vdots & \vdots & \vdots \\ 0 & 0 & \cdots & 1 & 0 & 0 & \cdots & 1 \end{bmatrix}^T$$

and let $\mathcal{R}(\Psi^P)$ be the range of Ψ^P. Then, $\mathcal{R}(\Psi^P)$ is the subspace of signals of period P and any other period $\bar{P}$ for which $\bar{P}$ is a factor of P. For single period estimation, the maximum likelihood (ML) estimate minimizes the two norm of the distance between R and $\mathcal{R}(\Psi^P)$ [12]. The ML estimate minimizes

$$\|R - \hat{S}\|^2 = \sum_{k=0}^{K_0-1} (r_k - \hat{s}_k)^2 \tag{1}$$

where $\hat{S}$ is the projection of R onto $\mathcal{R}(\Psi^P)$, which is the subspace corresponding to signals of period P (i.e., $\hat{s}_k = \hat{q}_{k \bmod P}$, and $\hat{q}_k = (1/M) \sum_{l=0}^{M-1} r_{k+lP} =< R, \psi_k >$). Minimizing (1) is equivalent to maximizing the square of the 2-norm of $\hat{S}$

$$\|\hat{S}\|^2 = \sum_{k=0}^{P-1} \langle R, \psi_k \rangle^2. \tag{2}$$

With $\phi_R(k)$, which is the unnormalized autocorrelation function of R, defined as

$$\phi_R(k) = \sum_{j=0}^{K_0-1-k} r_j r_{j+k}$$

it is shown in [12] that

$$\|\hat{S}\|^2 = \frac{P}{K_0} \left[\phi_R(0) + 2 \sum_{l=1}^{M-1} \phi_R(lP) \right]. \tag{3}$$

The first term in (3) $(P/K_0)\phi_R(0)$ grows linearly with P. In order to eliminate some of the bias toward larger periods, in [12], it is eliminated. The proposed period estimate in [12] is

$$\hat{P} = \arg\max_P \left\{ g_{(P,R)} = \frac{2P}{K_0} \sum_{l=1}^{M-1} \phi_R(lP) \right\} \tag{4}$$

and the signal estimates $\hat{k}_i$ for $i = 0, \ldots, \hat{P} - 1$ are

$$\hat{q}_k = \frac{1}{M} \sum_{l=0}^{M-1} r_{k+lP}$$

The algorithm of [12] is applied to a simple signal of length 12:

$$R_1 = [1, 2, 1, 2, 1, 2, 1, 2, 1, 2, 1, 2].$$

The graph of Fig. 1 represents the energy of the projections of R_1 onto the corresponding subspaces $\mathcal{R}(\Psi^k)$ calculated using (3). Notice the following.

1) Although the signal is of period 2, there is significant energy at period 1 (the dc value) and at period 3. This is due to the nonzero dc component and the fact that a dc signal is also periodic with period 3.
2) The signal has equal energy at period 2 and 4. It is not clear whether the signal is of period 2, or 4, or both. Every signal that is period 2 is also period 4, but not every signal of period 4 is of period 2.
3) The basis set $[\Psi^1 \Psi^2 \cdots \Psi^{P_{\max}}]$ is an over-complete set. Therefore, the sum of the energies onto $\mathcal{R}(\Psi^1), \mathcal{R}(\Psi^2), \ldots, \mathcal{R}(\Psi^{P_{\max}})$ is larger than the energy of the signal.

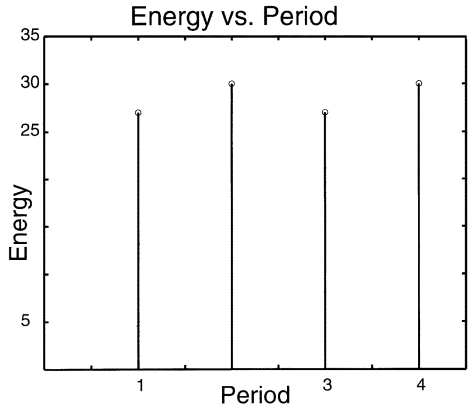

Fig. 1. Plot of the energy of the projections of R_1 onto the subspace $\mathcal{R}(\Psi^1), \ldots, \mathcal{R}(\Psi^4)$.

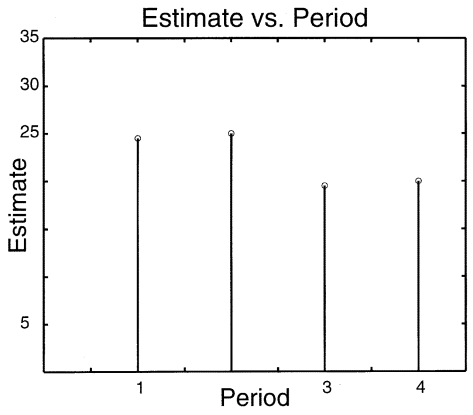

Fig. 2. Plot of the period estimate for R_1 using (4).

The graph of Fig. 2 represents the results of using the estimate in (4). The results are better, but the graph still shows significant energy at all periods. The challenge is to extend the results of [12] such that the ambiguities mentioned above are eliminated and to extend [12] to multiple periods. This is done in the next section.

III. Exactly Periodic Signals

As shown in the previous section, the approach of [12] has several drawbacks, the most serious of which is the inability to tell whether a signal is of period P or an integer multiple of P. For integer $n > 1$, the subspace $\mathcal{R}(\Psi^{nP})$ has a higher dimension than $\mathcal{R}(\Psi^P)$. If the signal contains noise, the projection of R onto $\mathcal{R}(\Psi^{nP})$ will always have more energy than the projection of R onto $\mathcal{R}(\Psi^P)$, and the method of [12] will always estimate a multiple of P. There is no direct way to tell how much

of the energy in $\mathcal{R}(\Psi^{nP})$ comes from signals of period P, how much from signals of period nP, and how much from signals of other periods that have a common divisor with nP. This difficulty stems from the fact that a signal of period P is also of a period that is a multiple of P. To eliminate this ambiguity, the following definition is introduced.

Definition 1: A signal S is of *exactly period* P if S is in $\mathcal{R}(\Psi^P)$, and the projection of S onto $\mathcal{R}(\Psi^{\bar{P}})$ is zero for all $\bar{P} < P$.

With this new definition, a signal of exactly period P is not exactly period $2P, 3P$, etc. although it continues to be of period $2P, 3P$, etc. In addition, not every periodic signal is exactly periodic, but every exactly periodic signal is periodic. The received signal R_1 is not exactly period 2 since the projection of R_1 onto $\mathcal{R}(\Psi^1)$ is not zero. Similarly, the signal is not exactly period 4 or exactly period 3. A signal that is exactly period 4 is

$$R_2 = [-1,-1,1,1,-1,-1,1,1,-1,-1,1,1].$$

To extend the results of [12] to multiple periods, let $S_1, \ldots, S_m$ be exactly periodic with periods $P_1, \ldots, P_m$, respectively. The received signal R of length K_0 (K_0 is a multiple of $P_1, \ldots, P_m$) then consists of $S_1, \ldots, S_m$ plus zero mean, white Gaussian noise $N \sim \mathcal{N}(0, \sigma^2)$

$$R = S_1 + \cdots + S_m + N.$$

With an unknown variance, the ML estimator maximizes the two norm of the sum of the estimates of the subsignals $(\hat{S}_1 + \cdots + \hat{S}_m)$, using estimates $\hat{\sigma}^2$ and $\hat{P}_1, \ldots, \hat{P}_m$. Assume that there exists orthogonal subspaces corresponding to signals of exactly periods $P_1, \ldots, P_m$, this task is easy. To obtain the norm squared of $(\hat{S}_1 + \cdots + \hat{S}_m)$, project R onto the m orthogonal subspaces to obtain estimates $\hat{S}_1, \ldots, \hat{S}_m$ and add their squared norms

$$\|\sum_i^m \hat{S}_i\|^2 = \sum_i^m \|\hat{S}_i\|^2.$$

In other words, projecting R onto orthogonal subspaces corresponding to signals of exactly period P (with P ranging from 1 to $P_{\max}$), the ML estimator of periods selects the m largest 2-norm projections. The next section deals with the existence of EPSs and their orthogonality.

IV. Exactly Periodic Subspace Decomposition (EPSD)

This section finds the subspaces corresponding to signals of exactly period P and shows that these subspaces are orthogonal to each other. The problem is studied in time and in frequency domain as each approach gives a slightly different insight into the problem.

A. Time Domain Interpretation

The study of this problem in the time domain begins with the following definition.

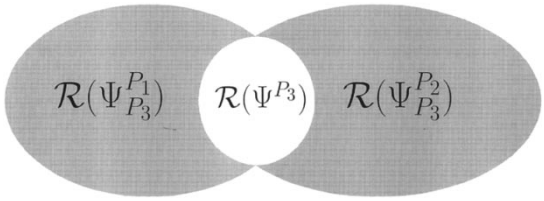

Fig. 3. Subspaces $\mathcal{R}(\Psi^{P_1}_{P_3})$, $\mathcal{R}(\Psi^{P_3})$, and $\mathcal{R}(\Psi^{P_2}_{P_3})$ are mutually orthogonal. $\mathcal{R}(\Psi^{P_1}) = \mathcal{R}(\Psi^{P_1}_{P_3}) \oplus \mathcal{R}(\Psi^{P_3})$, and $\mathcal{R}(\Psi^{P_2}) = \mathcal{R}(\Psi^{P_2}_{P_3}) \oplus \mathcal{R}(\Psi^{P_3})$.

Definition 2: Define $\Psi^P_{p_1,\ldots,p_m}$, with p_i divisors of P, to be the matrix whose range is the orthogonal complement of $\mathcal{R}[\Psi^{p_1} \cdots \Psi^{p_m}]$ inside $\mathcal{R}(\Psi^P)$:

$$\mathcal{R}\left(\Psi^P_{p_1,\ldots,p_m}\right) = \mathcal{R}(\Psi^P) \cap \left(\mathcal{R}\left[\Psi^{p_1} \cdots \Psi^{p_m}\right]\right)^{\perp}.$$

Since $\mathcal{R}(\Psi^{p_i}) \subset \mathcal{R}(\Psi^P)$, $\Psi^P_{p_1,\ldots,p_m}$ is not empty. If p_i are all the possible divisors of P, including 1, then $\mathcal{R}(\Psi^P_{p_1,\ldots,p_m})$ is the subspace corresponding to signals of exactly period P. To prove this, the following lemma is introduced.

Lemma 1: Given a signal R of length K_0 (K_0 is a multiple of P_1 and P_2), let $\mathcal{R}(\Psi^{P_1})$ be the subspace corresponding to period P_1 and $\mathcal{R}(\Psi^{P_2})$ be the subspace corresponding to period P_2. In addition, let $\mathcal{R}(\Psi^{P_3})$ be the subspace corresponding to period P_3, where P_3 is the greatest common divisor of P_1 and P_2. Then, $\mathcal{R}(\Psi^{P_3})$ is the intersection of $\mathcal{R}(\Psi^{P_1})$ and $\mathcal{R}(\Psi^{P_2})$. Moreover, the orthogonal complement of $\mathcal{R}(\Psi^{P_3})$ in $\mathcal{R}(\Psi^{P_1}), \mathcal{R}(\Psi^{P_1}_{P_3})$ is orthogonal to the orthogonal complement of $\mathcal{R}(\Psi^{P_3})$ in $\mathcal{R}(\Psi^{P_2}), \mathcal{R}(\Psi^{P_2}_{P_3})$. In other words, the three subspaces of Fig. 3 are mutually orthogonal.

Proof: Assume that the received signal R contains two periodic signals of periods P_1 and P_2 and that R is of length K_0 (K_0 a multiple of P_1 and $P_2, K_0 = P_1 M_1 = P_2 M_2$). Using the notation of Section II, $\mathcal{R}(\Psi^{P_1})$ and $\mathcal{R}(\Psi^{P_2})$ are two subspaces corresponding to signals of period P_1 (and any of the subdivisors of P_1) and signals of period P_2 (and any of the subdivisors of P_2), respectively. For the sake of clarity, let $P_1 = 4$ and $P_2 = 6$. By definition, Ψ^{P_1} and Ψ^{P_2} are

$$\Psi^{P_1} = c_1 \begin{bmatrix} 1000\cdots \\ 0100\cdots \\ 0010\cdots \\ 0001\cdots \end{bmatrix}^T, \quad \Psi^{P_2} = c_2 \begin{bmatrix} 100000\cdots \\ 010000\cdots \\ 001000\cdots \\ 000100\cdots \\ 000010\cdots \\ 000001\cdots \end{bmatrix}^T$$

with $c_1 = (1/\sqrt{M_1})$ and $c_2 = (1/\sqrt{M_2})$. Let P_3 be the greatest common divisor of P_1 and P_2. Any signal of period P_3 is in both $\mathcal{R}(\Psi^{P_1})$ and $\mathcal{R}(\Psi^{P_2})$. In other words, $\mathcal{R}(\Psi^{P_3}) \subset [\mathcal{R}(\Psi^{P_1}) \cap \mathcal{R}(\Psi^{P_2})]$. Next, any signal in $\mathcal{R}(\Psi^{P_1})$ must be of some period $\hat{P}_1$, with $\hat{P}_1$ a divisor of P_1, and any signal in $\mathcal{R}(\Psi^{P_2})$ must be of some period $\hat{P}_2$, with $\hat{P}_2$ a divisor of P_2. Therefore, any signal that is in both $\mathcal{R}(\Psi^{P_1})$ and $\mathcal{R}(\Psi^{P_2})$ must be of period $\hat{P}$, for which $\hat{P}$ is a divisor of both P_1 and P_2. In particular, $\hat{P}$ is a divisor of P_3, and any signal that is in both $\mathcal{R}(\Psi^{P_1})$ and $\mathcal{R}(\Psi^{P_2})$ must be in $\mathcal{R}(\Psi^{P_3})$ or $[\mathcal{R}(\Psi^{P_1}) \cap \mathcal{R}(\Psi^{P_2})] \subset \mathcal{R}(\Psi^{P_3})$. Thus, the intersection of $\mathcal{R}(\Psi^{P_1})$ and $\mathcal{R}(\Psi^{P_2})$ is $\mathcal{R}(\Psi^{P_3})$, as shown in Fig. 3.

Next, find subspaces $\mathcal{R}(\Psi^{P_1}_{P_3}), \mathcal{R}(\Psi^{P_2}_{P_3})$ and $\mathcal{R}(\Psi^{P_3})$ such that $\mathcal{R}(\Psi^{P_1}) = \mathcal{R}(\Psi^{P_1}_{P_3}) \oplus \mathcal{R}(\Psi^{P_3})$ and $\mathcal{R}(\Psi^{P_2}) = \mathcal{R}(\Psi^{P_2}_{P_3}) \oplus \mathcal{R}(\Psi^{P_3})$. The claim is that subspaces $\mathcal{R}(\Psi^{P_1}_{P_3}), \mathcal{R}(\Psi^{P_2}_{P_3})$ and $\mathcal{R}(\Psi^{P_3})$ are

$$\mathcal{R}\left(\Psi^{P_3}\right) = \mathcal{R}\left(\Psi^{P_1}\right) \cap \mathcal{R}\left(\Psi^{P_2}\right) \tag{5}$$

$$= \mathcal{R}\left[\Psi^{P_1}\left(\Psi^{P_1}\right)^T \Psi^{P_2}\right] \tag{6}$$

$$= \mathcal{R}\left[\Psi^{P_2}\left(\Psi^{P_2}\right)^T \Psi^{P_1}\right] \tag{7}$$

$$\mathcal{R}\left(\Psi^{P_1}_{P_3}\right) = \mathcal{R}\left[\Psi^{P_1} - \Psi^{P_2}\left(\Psi^{P_2}\right)^T \Psi^{P_1}\right] \tag{8}$$

$$\mathcal{R}\left(\Psi^{P_2}_{P_3}\right) = \mathcal{R}\left[\Psi^{P_2} - \Psi^{P_1}\left(\Psi^{P_1}\right)^T \Psi^{P_2}\right]. \tag{9}$$

The proof of (6) and (7) is left for the Appendix. To prove(8) and (9), it is enough to show that $\mathcal{R}[\Psi^{P_1} - \Psi^{P_2}(\Psi^{P_2})^T\Psi^{P_1})]$ is the orthogonal complement of $\mathcal{R}(\Psi^{P_3})$ in $\mathcal{R}(\Psi^{P_1})$ and that $\mathcal{R}[\Psi^{P_2} - \Psi^{P_1}(\Psi^{P_1})^T\Psi^{P_2}]$ is the orthogonal complement of $\mathcal{R}(\Psi^{P_3})$ in $\mathcal{R}(\Psi^{P_2})$.

Clearly, any signal in $\mathcal{R}(\Psi^{P_1})$ can be written as a linear combination of vectors in $\mathcal{R}[\Psi^{P_1} - \Psi^{P_2}(\Psi^{P_2})^T\Psi^{P_1}]$ and vectors in $\mathcal{R}(\Psi^{P_3}) = \mathcal{R}[\Psi^{P_2}(\Psi^{P_2})^T\Psi^{P_1}]$ and similarly for $\mathcal{R}(\Psi^{P_2})$. All that is left is to show that

$$\mathcal{R}\left[\Psi^{P_1} - \Psi^{P_2}\left(\Psi^{P_2}\right)^T \Psi^{P_1}\right] \perp \mathcal{R}\left(\Psi^{P_3}\right) \tag{10}$$

$$\mathcal{R}\left[\Psi^{P_2} - \Psi^{P_1}\left(\Psi^{P_1}\right)^T \Psi^{P_2}\right] \perp \mathcal{R}\left(\Psi^{P_3}\right). \tag{11}$$

The first orthogonality is true since $(\Psi^{P_2})^T \times (\Psi^{P_1} - \Psi^{P_2}(\Psi^{P_2})^T\Psi^{P_1}) = 0$, and $\mathcal{R}(\Psi^{P_3}) \subset \mathcal{R}(\Psi^{P_2})$. It is similar for the second orthogonality. In other words

$$\mathcal{R}\left(\Psi^{P_1}_{P_3}\right) \perp \mathcal{R}\left(\Psi^{P_2}\right) \Rightarrow \mathcal{R}\left(\Psi^{P_1}_{P_3}\right) \perp \mathcal{R}\left(\Psi^{P_2}_{P_3}\right). \tag{12}$$

This completes the proof. ■

The next two theorems prove the orthogonality of subspaces corresponding to signals of exactly period P.

Theorem 1: For any two specific periods P and $U(P \neq U)$ and signal R of length K_0 (K_0 a multiple of P and U), let $p_1, \ldots, p_n$ and $u_1, \ldots, u_m$ be all the possible divisors of P and U, respectively (this includes 1 and excludes P and U, respectively). Then, $\mathcal{R}(\Psi^P_{p_1,\ldots,p_n})$ and $\mathcal{R}(\Psi^U_{u_1,\ldots,u_m})$ are orthogonal.

Proof: Without loss of generality, let $p_1 = u_1$ be the greatest common divisor of P and U. Then, $\mathcal{R}(\Psi^P_{p_1,\ldots,p_n}) \subset \mathcal{R}(\Psi^P_{p_1})$ and $\mathcal{R}(\Psi^U_{u_1,\ldots,u_m}) \subset \mathcal{R}(\Psi^U_{u_1})$. By Lemma 1, $\mathcal{R}(\Psi^P_{p_1})$ is orthogonal to $\mathcal{R}(\Psi^U_{u_1})$. ■

The next theorem proves that the subspace corresponding to signals of exactly period P is $\mathcal{R}(\Psi^P_{p_1,\ldots,p_n})$.

Theorem 2: Let $p_1, \ldots, p_n$ be all the possible divisors of P (including 1 but not P). Then, S is exactly period P if and only if $S \in \mathcal{R}(\Psi^P_{p_1,\ldots,p_n})$.

Proof: First, assume that $S \in \mathcal{R}(\Psi^P_{p_1,\ldots,p_n})$. For any period $\bar{P} < P$, $\bar{P}$ and P have a greatest common divisor (which can also be $\bar{P}$ itself or 1). Without loss of generality, let p_1 be the greatest common divisor of $\bar{P}$ and P. From Theorem 1, $\mathcal{R}(\Psi^P_{p_1})$ is orthogonal to $\mathcal{R}(\Psi^{\bar{P}})$. With $\mathcal{R}(\Psi^P_{p_1,\ldots,p_n}) \subset \mathcal{R}(\Psi^P_{p1}), \mathcal{R}(\Psi^P_{p_1,\ldots,p_n})$ is orthogonal to $\mathcal{R}(\Psi^{\bar{P}})$. In other words, the projection of $S \in \mathcal{R}(\Psi^P_{p_1,\ldots,p_n})$ onto $\mathcal{R}(\Psi^{\bar{P}})$ is zero for all $\bar{P} < P$, and S is exactly period P.

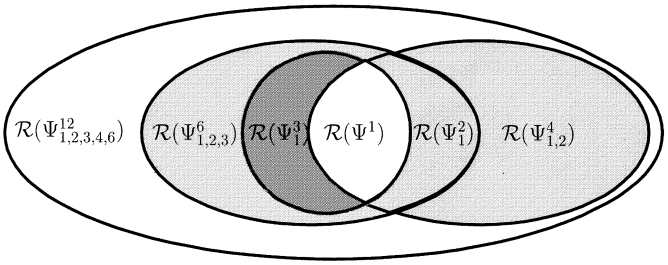

Fig. 4. Subspaces $\mathcal{R}(\Psi^{12}_{1,2,3,4,6}), \mathcal{R}(\Psi^{6}_{1,2,3}), \mathcal{R}(\Psi^{3}_{1}), \mathcal{R}(\Psi^{1}), \mathcal{R}(\Psi^{2}_{1})$, and $\mathcal{R}(\Psi^{4}_{1,2})$ are mutually orthogonal. Together, they span the entire subspace $\mathcal{R}(\Psi^{12})$.

Second, assume that S is exactly period P. By definition, $S \in \mathcal{R}(\Psi^P)$ and $S \perp \mathcal{R}(\Psi^{\bar{P}})$ for any $\bar{P} < P$. In other words, S is in the orthogonal complement of $\mathcal{R}[\Psi^{p_1}, \ldots, \Psi^{p_n}]$ inside $\mathcal{R}(\Psi^P)$. Therefore, $S \in \mathcal{R}(\Psi^P_{p_1,\ldots,p_n})$. ■

A simple example is to find the basis of all EPSs included in $\mathcal{R}(\Psi^{12})$. In other words, find the subspaces that span signals of exactly period 12, exactly period 6, exactly period 4, exactly period 3, exactly period 2, and exactly period 1, as shown in Fig. 4. To find the subspace of exactly period 2, subtract the projection of the subspace $\mathcal{R}(\Psi^2)$ onto $\mathcal{R}(\Psi^1)$, from $\mathcal{R}(\Psi^2)$. Proceed with the other EPSs in a similar fashion. The subspaces of (13), shown at the bottom of the next page, are obtained by repeated use of (8) and (9). (The interested reader is encouraged to use the code from [15].) Notice how each of the six subspaces are mutually orthogonal. For example, the basis vectors of $\mathcal{R}(\Psi^6_{1,2,3})$ are of period six but not of period 1, 2, or 3. It is also interesting to note that (8) and (9) resemble something of a Gram–Schmidt decomposition for subspaces. What is interesting is that the intersection of the two subspaces can be written as either (6) or (7). In general, the intersection, as shown by (13), of two subspaces is not described by (6) or (7). This works only because of the special structure of the subspaces, as shown in Appendix.

1) Calculation of Orthogonal Projections: This section discusses the computation of the projection of R onto the orthogonal subspaces corresponding to exactly period P. For this purpose, (3) can be used directly without ever explicitly forming the subspaces corresponding to exactly period P. Again, let $p_1, \ldots, p_n$ be all the possible divisors of P (including 1 and not P). For $P = 12$, all the possible factors of 12 are 1, 2, 3, 4, and 6. Let the function *AllPossibleFactors* be a function that returns all these factors $p_1 \ldots p_n$ given P. By definition, the subspace corresponding to signals of exactly period P is the orthogonal complement of the union of the subspaces corresponding to exactly period p_i inside $\mathcal{R}(\Psi^P)$. Theorem 1 then guarantees that

$$\mathcal{R}(\Psi^P) = \text{subspace of exactly period } P \oplus \sum_{\oplus} \text{subspace of exactly period } p_i. \tag{14}$$

Using Matlab notation, the algorithm for calculating the projections and the dimensions of each EPS is depicted in Table I. More concretely, in the example of Fig. 4, to find the projection onto $\mathcal{R}(\Psi^{12}_{1,2,3,4,6})$, first find the projections onto $\mathcal{R}(\Psi^6_{1,2,3}), \mathcal{R}(\Psi^3_1), \mathcal{R}(\Psi^1), \mathcal{R}(\Psi^2_1), \mathcal{R}(\Psi^4_{1,2})$ and then subtract them from $\mathcal{R}(\Psi^{12})$. To find the projection onto $\mathcal{R}(\Psi^3_1)$, subtract

TABLE I
ALGORITHM FOR CALCULATING THE PROJECTIONS ONTO EXACTLY PERIODIC SUBSPACES.

Calculating EPS Projections
% Array 'g' is calculated using equation (3)
ExactlyPeriodicEnergy(1)=g(1);
ExactlyPeriodicDimension(1)=1;
for P=2:P_{max},
% AllPossibleFactors(12) returns
% fact=[1,2,3,4,6];
fact=AllPossibleFactors(P);
ExactlyPeriodicEnergy(P) = ...
g(P)-sum(ExactlyPeriodicEnergy(fact));
ExactlyPeriodicDimension(P) = ...
P-sum(ExactlyPeriodicDimension(fact));
end

the projection onto $\mathcal{R}(\Psi^1)$ from the projection onto $\mathcal{R}(\Psi^3)$, and so on, for the other projections.

B. Frequency Domain Interpretation

Viewing the problem in the frequency domain reveals a very fast algorithm for computing the EPS projections. Any signal of period P can be written as a linear combination of the harmonics at frequencies $0, (1/P), (2/P), \ldots, (P-1)/(P)$. The harmonics at these frequencies form an orthonormal basis set for the subspace $\mathcal{R}(\Psi^P)$. The energy of the projection of R onto $\mathcal{R}(\Psi^P)$ can be calculated by summing up the squared magnitudes of the Fourier coefficients corresponding to all harmonics of the fundamental frequency $(1/P)$. Formally, using the notation of Section II and with $\tilde{R}$ as the Fourier transform of R, this means

$$\|\hat{S}\|^2 = \sum_{k=0}^{P-1} \left| \langle R, e^{j(\frac{2\pi}{Nk_0})(\frac{k_0}{P})k} \rangle \right|^2 = \sum_{k=0}^{P-1} \left| \tilde{R}\left(\frac{Nk_0}{P}\right) \right|^2. \quad (15)$$

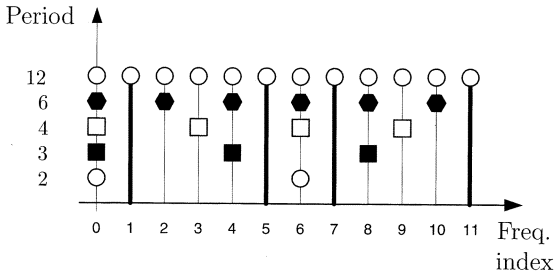

Fig. 5. Frequency of different periodic signals. The subspace of exactly periodic signals with period 12 is the collection of harmonics that belong only to period 12 (i.e., the harmonics with $k = 1, 5, 7$, and 11).

This is the equivalent of (3) in the frequency domain. To find the projection of R onto the EPS of period P, only a subset of the harmonics $0, (1)/(P), (2)/(P), \ldots, (P-1)/(P)$ is summed up. Going back to the example of (13) in the frequency domain, the basis functions for $\mathcal{R}(\Psi^{12})$ are the harmonics $e^{j((2\pi k)/(12))}$ with $k = 0, \ldots, 11$. The basis function for $\mathcal{R}(\Psi^1)$ is the harmonic with $k = 0$. For $\mathcal{R}(\Psi^2)$, the basis is the harmonics with $k = 0, 6$ and similarly for $\mathcal{R}(\Psi^3), k = 0, 4, 8$; for $\mathcal{R}(\Psi^4), k = 0, 3, 6, 9$; and for $\mathcal{R}(\Psi^6), k = 0, 2, 4, 6, 8, 10$, as depicted in Fig. 5. The harmonics spanning the subspace of exactly period 12 signals $\mathcal{R}(\Psi^{12}_{1,2,3,4,6})$ are the harmonics with $k = 1, 5, 7, 11$.

In general, the basis functions for the subspace of exactly period P signals is spanned by the harmonics that are at multiples of the fundamental frequency $(1/P)$ but are not multiples of any frequency $1/\bar{P}$ with $\bar{P} \mid P$. The algorithm of Table II is the algorithm of Table I translated in the frequency domain.

C. EPSD Properties and Discussions

The EPSD is a complete decomposition. Any signal $R \in \mathbb{R}^n$ can be completely decomposed into exactly periodic orthogonal components corresponding to each of the EPSs of n and *AllPossibleFactors*(n). This is obvious from (14) since $\mathcal{R}(\Psi^n) = \mathbb{R}^n$ when $R \in \mathbb{R}^n$. This also means that the sum of two exactly periodic signals will not be exactly periodic unless the two signals are exactly periodic with the same period.

$$\Psi^1 = \frac{1}{\sqrt{12}}[1 \;\; 1 \;\; 1 \;\; 1 \;\; 1 \;\; 1 \;\; 1 \;\; 1 \;\; 1 \;\; 1 \;\; 1 \;\; 1]^T$$

$$\Psi^2_1 = \frac{1}{\sqrt{12}}[1 \;\; -1 \;\; 1 \;\; -1 \;\; 1 \;\; -1 \;\; 1 \;\; -1 \;\; 1 \;\; -1 \;\; 1 \;\; -1]^T$$

$$\Psi^3_1 = \frac{1}{\sqrt{24}} \begin{bmatrix} 2 & -1 & -1 & 2 & -1 & -1 & 2 & -1 & -1 & 2 & -1 & -1 \\ -1 & 2 & -1 & -1 & 2 & -1 & -1 & 2 & -1 & -1 & 2 & -1 \end{bmatrix}^T$$

$$\Psi^4_{1,2} = \frac{1}{\sqrt{6}} \begin{bmatrix} 1 & 0 & -1 & 0 & 1 & 0 & -1 & 0 & 1 & 0 & -1 & 0 \\ 0 & 1 & 0 & -1 & 0 & 1 & 0 & -1 & 0 & 1 & 0 & -1 \end{bmatrix}^T$$

$$\Psi^6_{1,2,3} = \frac{1}{\sqrt{24}} \begin{bmatrix} 2 & 1 & -1 & -2 & -1 & 1 & 2 & 1 & -1 & -2 & -1 & 1 \\ 1 & 2 & 1 & -1 & -2 & -1 & 1 & 2 & 1 & -1 & -2 & -1 \end{bmatrix}^T$$

$$\Psi^{12}_{1,2,3,4,6} = \frac{1}{\sqrt{12}} \begin{bmatrix} 2 & 0 & 1 & 0 & -1 & 0 & -2 & 0 & -1 & 0 & 1 & 0 \\ 0 & 2 & 0 & 1 & 0 & -1 & 0 & -2 & 0 & -1 & 0 & 1 \\ 1 & 0 & 2 & 0 & 1 & 0 & -1 & 0 & -2 & 0 & -1 & 0 \\ 0 & 1 & 0 & 2 & 0 & 1 & 0 & -1 & 0 & -2 & 0 & -1 \end{bmatrix}^T \quad (13)$$

TABLE II
ALGORITHM FOR CALCULATING THE PROJECTIONS ONTO EXACTLY PERIODIC SUBSPACES IN THE FREQUENCY DOMAIN

EPS in the Frequency Domain
$\tilde{R}$=FFT(R);
$\tilde{R}_E$=vector with energy of each $\tilde{R}$ coefficient;
for P=2:P_{max},
% with any $\bar{P}\|P$
$fact$=harmonics multiple of $1/P$,
but not multiple of $1/\bar{P}$
ExactlyPeriodicEnergy(P) = sum($R_E(fact)$);
end

If $R \in \mathbb{R}^{12}$, the signal is decomposed into signals of exactly period 1, 2, 3, 4, 6, and 12. Just like the Fourier decomposition, the EPSD decomposes the signal into orthogonal components. Unlike the Fourier transform, the EPSD is obtained by taking projections onto exactly periodic orthogonal multidimensional subspaces of periods that divide n, whereas the discrete Fourier transform is obtained by taking orthogonal projections onto one-dimensional (1-D) complex exponentials $e^{j((2\pi)/N)k}$ with frequencies $(k/N), \mathrm{k} = 0, \ldots, \mathrm{N}-1$. The EPS is spanned by a collection of Fourier exponentials, which is dictated by the period. When searching for periodic components, this is the main advantage of the EPSD. By having subspaces of dimensions larger than one, the EPS can better capture, in one coefficient, the periodic energy than can the Fourier transform. Unlike the method of summing up all the harmonics to each fundamental frequency [12], the EPS does not leave any ambiguity about the period of the signal. It does not estimate a multiple of the period, as [12] does, especially when noise is added.

Mathematically, a signal of length 12 can have subsignals of only periods 1, 2, 3, 4, 6, and 12. Looking for an exactly period 5 signal in a length 12 signal is done by assuming that the first ten samples repeat periodically. (If this assumption is not made, then there will be leakage effects similar to the Fourier transform, which is outside the scope of this paper.) A signal of exactly period 5 is orthogonal to a signal of exactly period 6 as long as they have the same length. In other words, both signals are of length multiple of 30, which is the least common multiplier of 5 and 6. When searching for periodic subsignals, the search needs to include periods that do not necessarily divide the length of R. It turns out that as long as there is at least one period in R, the EPSD can successfully recover one period of the exactly periodic subsignal with the assumption that signals repeat periodically, as above.

When decomposing the signal into EPSs of periods that divide the length of R, the EPSD coefficients represent the different exactly periodic energies. The square root of the sum of the squares of the EPSD coefficients is the r.m.s. value of the signal R. Using EPSD to decompose the signal into exact periods of 1, through some $P_{\max}$, the sum of the squares of the EPSD coefficients no longer adds up to the squared norm of R unless all the periods less than $P_{\max}$ divide the length of R, and there are no exactly periodic signals of periods larger than $P_{\max}$. While the energy no longer sums up to the energy of R, if $P_{\max}$ is much smaller than the length of R, the coefficients still represent a good approximation of the exactly periodic signals had the signal R been extended such that all the EPSs up to period $P_{\max}$ would be orthogonal.

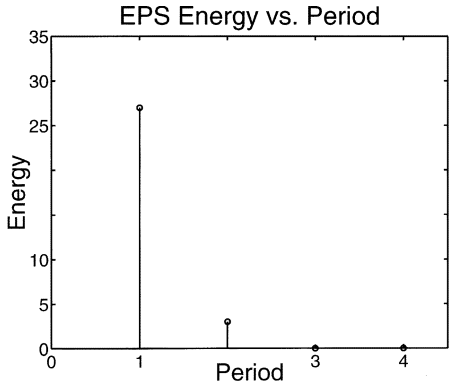

Fig. 6. Plot of the energy of the projections of R_1, from Section II, onto EPSs.

Finally, the energy of the projection of white noise on the EPSs is proportional to the dimension of the EPS. If the desire is to have an estimator such that for white noise no period is reported stronger than any other, then the energy of the projection of the signal on the EPS of period P should be divided by the dimension of the subspace. (Note that the dimension of the EPS is always smaller than P. When P is a prime number the dimension is $P-1$.)

V. EPS EVALUATION

A. Synthetic Signals

The first example compares the method of [12], which is equivalent to summing up all harmonics to each fundamental frequency (15), to the new EPSD. The plot of Fig. 6 is obtained using the EPSD on the signal R_1 of Section II. The signal contains a subsignal of exactly period 1 and a subsignal of exactly period 2. There are no subsignals of exactly period 3 or exactly period 4. The subsignal of exactly period 1 is the dc component. In Fig. 1, the fact that a dc signal is also considered to be of period 3 causes ambiguity in readings. From Fig. 1, it is not immediately clear whether or not there is a hidden subsignal that is truly periodic, with period 3. That ambiguity is removed in Fig. 6. With the introduction of the concept of exactly periodic signals, it is now obvious that there are no subsignals that are of exactly period 3. The idea of exactly periodic signals makes sense. A dc signal is not usually thought of as being of period three.

The second example is a synthetic signal generated by adding ramp signals of periods 6, 36, and 45. The ramp signals, in Matlab notation, are $x_6 = [1:6, 1:6, \ldots], x_{36} = [1:36, 1:36, \ldots]$, and $x_{45} = [1:45, 1:45, \ldots]$. The least common multiplier of 6, 36, and 45 is 180. To add these signals together, the signal length must be a multiple of 180. The signal length is $4320 = 180 \times 24$, with the number of repetitions (24) being chosen arbitrarily. For convenience, the mean is taken out. The energy distribution obtained from the M-Best gamma corrected algorithm of [8] (Matlab program *mbestgam.m* of [16]) is depicted in Fig. 7, whereas the energy distribution using EPSD is depicted in Fig. 8. Both algorithms predict large signal components of periods 36 and 45. Due to the order of projections in

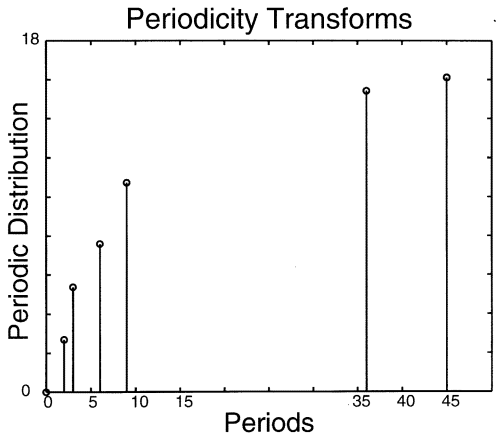

Fig. 7. Period distribution estimated using the M-Best algorithm periodicity transform.

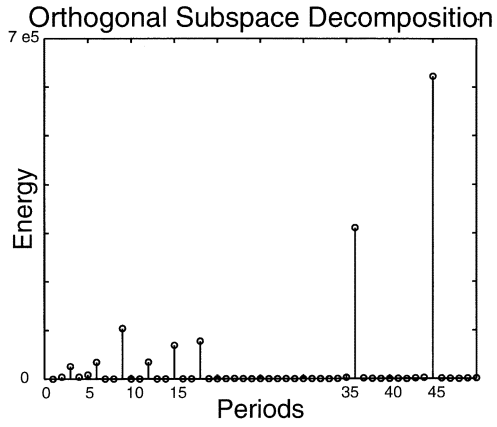

Fig. 8. Periodic energy using EPSD.

[8], a signal of exactly period 15 is considered to be of period 45. This is correct since a signal of exactly period 15 is also of period 45. However, a signal of exactly period 15 is not exactly period 45. This is the main difference between the two algorithms. The EPSD predicts high energy in the signal of exactly period 15, whereas the algorithm of [8] combines the exactly period 15 signal with the exactly period 45 signal to obtain a new periodic signal of period 45. The combined signal is no longer of exactly period 45. The synthetic signal contains signals of exactly period 12, 15, and 18. Moreover, the signals of exactly period 18 are larger than the signals of exactly period 2, as depicted in Fig. 8. The periodicity transform of [8] detects subsignals of period 2 but does not detect subsignals of exactly period 18, which in fact are larger than the signals of exactly period 2. The EPS decomposes the synthetic signal into signals of exactly period 2, 3, 4, 5, 6, 9, 12, 15, 18, 36, and 45. When added together, the exactly periodic signals completely reconstruct the synthetic signal, and the decomposition is unique.

The third example compares the Fourier decomposition with the EPSD. A random signal of 320 samples is projected onto the EPS of period 32, and the result is repeated ten times to generate a periodic signal S, with period 32. Fig. 9 depicts the magnitudes of the Fourier coefficients (a) of the synthetic signal S (c). With zero noise the frequency peaks are identified at multiples of $1/P(P = 32)$. The EPSD [Fig. 9(b)] also clearly indicates large energy at period 32. After adding noise, the magnitude plot of the Fourier coefficients [Fig. 10(a)] is no longer as useful in estimating the period. Searching for the largest peak, the period is estimated at $32/4$, whereas the EPSD continues to correctly identify the largest periodic energy to be at 32 [Fig. 10(b)]. The estimate of $\hat{S}$ is obtained from the EPSD and is plotted together with the original signal in Fig. 10(c). Unless the signal is a sinusoid, the Fourier transform has frequency peaks at multiples of $1/P$. In this example, the signal has larger frequency response at higher frequencies. Searching for the largest peak in the frequency response estimates a multiple of the period. Things get even more complicated when there are multiple periodic signals, for it is no longer clear what frequency peaks belong to what period.

B. Vibration Data Signals

This section discusses the application of EPSD to real data vibration signals. One difficulty with almost any period estimation method is that the period of the analog signal does not contain an integer number of samples. The sampled data is never periodic. One approach to solving this problem is to force an integer number of samples per period by doing synchronous sampling. Instead of sampling the vibration signal using a fixed frequency clock, sampling is synchronized with the position of the gears. The intuition is that interesting subsignals are generated by defects in the gears and occur periodically at the same location relative to the position of the gears. Therefore, synchronous sampling provides an integer number of samples for these periodic subsignals. Fig. 11 contains the plot of $g_{(P,R)}$, (4), calculated from vibration data obtained with synchronous sampling (b) and from vibration data obtained with a fixed 25-kHz sampling clock (c). The difference in the performance of the two approaches is obvious. Synchronous sampling gives almost ideal results on real vibration data, whereas using conventional sampling is less satisfactory. Using a fixed clock sampling rate, the peaks corresponding to $g(P, R)$ are not as well defined as in the synchronous case.

The EPSD is applied to a real data vibration signal recorded from a General Motor gear box; see Fig. 11(a). The signal length is $32\,768 = 2^{15}$, which is equivalent to 32 revolutions of the large wheel in Fig. 11(a). The energy distribution shown in Fig. 12(a) is obtained by applying the EPSD to the vibration data. The first two peaks are at periods 164 and 329. Interestingly, $164 \times 2 = 328$, which seems to suggest that the signal of period 329 is nothing else but a duplicate of the signal of period 164. Nonetheless, the signal of exactly period 329 is not a repeat of the signal of exactly period 164, and the signal of exactly period 329 is orthogonal with the signal of exactly period 164 when the length of the signal is a multiple of 53 956, which is the least common multiplier of 329 and 164.

The sampling frequency is 1024 samples per revolution, and the gear box has 1750 r/min. This is equivalent to about 29-kHz sampling rate, which means that a signal of 60 Hz has about 497 samples per cycle. This means that there are 248 and 166 samples per cycle for the second and third harmonic, respectively.

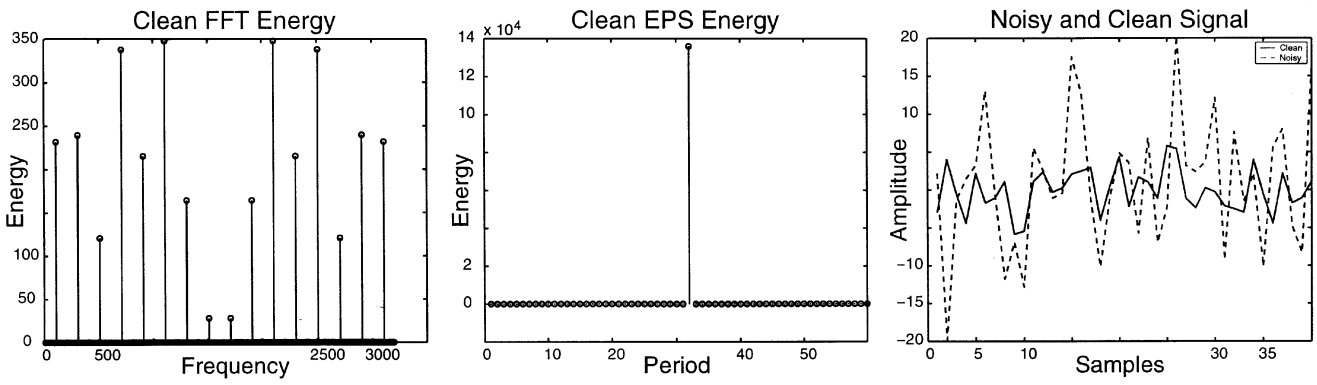

(a) (b) (c)

Fig. 9. (a) Fourier coefficients energy of S. (b) EPS periodic energy of S. (c) Portion of the clean signal S plotted together with the received noisy signal $R = S + N$.

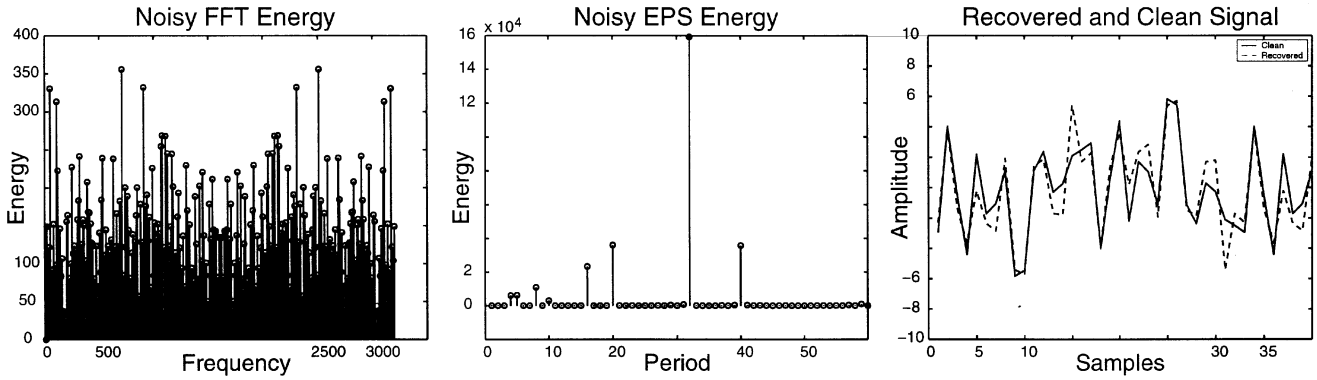

(a) (b) (c)

Fig. 10. (a) Fourier coefficients energy of R. (b) EPS periodic energy of R. (c) Portion of the clean signal S plotted together with the recovered signal $\hat{S}$.

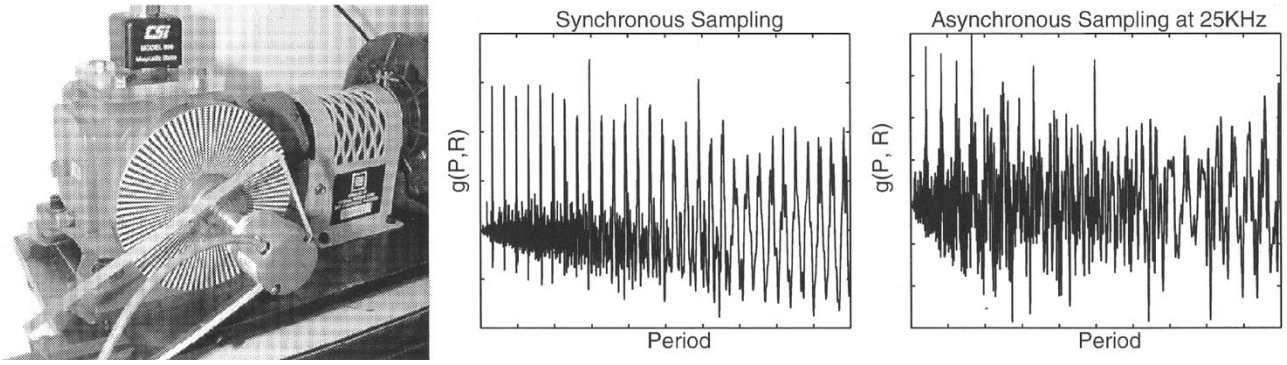

(a) (b) (c)

Fig. 11. (a) General Motors gear box used for the real time synchronous sampling. (b) Plot of $g(P, R)$ for synchronous sampling. (c) Plot of $g(P, R)$ for 25-kHz, asynchronous sampling.

In Fig. 12(a), there are large peaks at 493 and 164. This suggests that some of the large peaks are due to the electrical noise pickup in the system.

In calculating the energy distribution, most of the computation is spent on (3). The autocorrelation function can be calculated efficiently using the fast Fourier transform. In Matlab, on a 700-MHz Pentium III, the EPSD spends a little less than 2 min on 32 768 points of vibration data. Using the method presented in [8] takes much longer. Using a C implementation, the period estimation program runs in real time (using a window of about 4000 data points) analyzing vibration data using the gear box of Fig. 11(a).

VI. Conclusion

This paper introduced the concept of exactly periodic signals and EPSs. Through examples it compared this new approach to the Fourier transform and the period estimation approach of [8], emphasizing the advantages of the new method. The EPSD is done by projecting the signal onto orthogonal EPSs, which is similar to Fourier and wavelet decompositions. The difference, however, is that unlike the Fourier or wavelet decomposition, which take projections onto orthogonal vectors, the EPSD takes projections onto orthogonal subspaces.

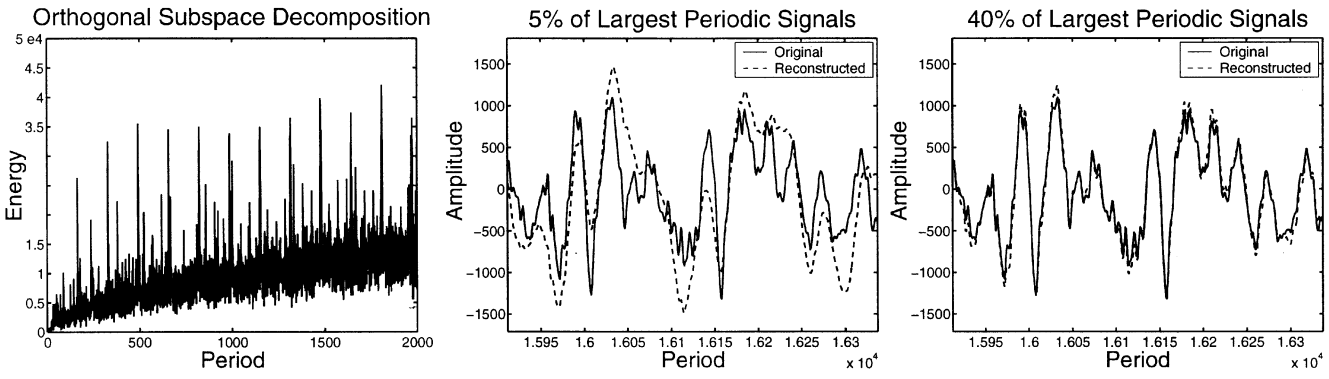

(a) (b) (c)

Fig. 12. (a) Exactly periodic energy of the gear box vibration signal. Plot of the original vibration signal together with the sum of the first (b) 5 and (c) 40% of the largest periodic signals.

APPENDIX
PROOF OF (6) AND (7)

This Appendix is concerned with the proof of (6) and (7)

$$\begin{aligned}\mathcal{R}(\Psi^{P_3}) &= \mathcal{R}(\Psi^{P_1}) \cap \mathcal{R}(\Psi^{P_2}) \\ &= \mathcal{R}[\Psi^{P_1}(\Psi^{P_1})^T\Psi^{P_2}] \\ &= \mathcal{R}[\Psi^{P_2}(\Psi^{P_2})^T\Psi^{P_1}]\end{aligned}$$

of Section IV. The key idea is that although the number of columns of the matrices $[\Psi^{P_1}(\Psi^{P_1})^T\Psi^{P_2}]$ and $[\Psi^{P_2}(\Psi^{P_2})^T\Psi^{P_1}]$ is not the same, the columns of the two matrices span the same subspace. To proves this the following claim is needed.

Claim 1: Let x and y be two relatively prime numbers. Form two vectors v_1 and v_2, both of length $l = x \times y$ (l is the least common multiplier), such that vector v_1 is formed by repeating the length x sequence $\{1,0,0,\ldots,0\}, y$ times, and vector v_2 is formed by repeating the length y sequence $\{1,0,0,\ldots,0\}, x$ times. Then, the dot product of v_1 and v_2 is one. Moreover, the dot product between any v_1' and v_2' (where v_1' and v_2' are circular shifted versions of v_1 and v_2, respectively) is also one.

Proof: To get an intuitive idea, here is an example:

Period 4 sequence: $v_1' = 100010001000$

Shifted period 3 sequence: $v_2' = 001001001001.$

The proof is showing that a 1 from the first vector matches with a 1 from the second vector one and only one time. Instead of thinking of vectors, let us think of sequences of numbers. The first sequence of numbers is v_1', and the second is v_2'.

First, a 1 from the v_1' sequence matches with a 1 from the second sequence v_2'. To see this assume the first sequence is shifted $d-1$. Then, a 1 is at position $d+nx$ for integer n. If the second sequence is shifted by $c-1$, then a 1 is at position $c+my$ for integer m. To have a match, it must be shown that $d+nx = c+my$ for some integers m, n or, equivalently

$$d - c = -nx + my.$$

(With the length of the two sequences as the product of x and y, there is no need to worry about any mod restrictions on m and n. All possible matchings happen in the first l positions, and everything starts repeating after that.)

Since x and y are relatively prime, there exist integers a and b such that $ax + by = 1$. Hence

$$\begin{aligned}d - c &= (d-c)(ax+by) \\ &= (d-c)ax + (d-c)by = -nx + my.\end{aligned}$$

Therefore, there is at least one matching of ones. To see that there will not be two matchings is also quite trivial. Matchings of 1s cannot be less than l apart. If they happened sooner, say $k < l$, then $x \mid k$ and $y \mid k$ (recall that the distance between consecutive 1s in the two sequences is x and y, respectively). This contradicts the fact that x and y are relatively prime. ■

Next, matrices Ψ^{P_1} and Ψ^{P_2} can be written as

$$\Psi^{P_1} = \begin{bmatrix} I_{P_1} \\ I_{P_1} \\ \vdots \\ I_{P_1} \end{bmatrix}_{K_0 \times P_1} \quad \text{and} \quad \Psi^{P_2} = \begin{bmatrix} I_{P_2} \\ I_{P_2} \\ \vdots \\ I_{P_2} \end{bmatrix}_{K_0 \times P_2}$$

where in Ψ^{P_1}, the identity matrix I_{P_1} repeats M_1 times, and in Ψ^{P_2}, the identity matrix I_{P_2} repeats M_2 times. Then

$$\Psi^{P_1}\left(\Psi^{P_1}\right)^T\Psi^{P_2} = \begin{bmatrix} I_{P_1} & \cdots & I_{P_1} \\ \vdots & \vdots & \vdots \\ I_{P_1} & \cdots & I_{P_1} \end{bmatrix}\begin{bmatrix} I_{P_2} \\ \vdots \\ I_{P_2} \end{bmatrix} \tag{16}$$

and

$$\Psi^{P_2}\left(\Psi^{P_2}\right)^T\Psi^{P_1} = \begin{bmatrix} I_{P_2} & \cdots & I_{P_2} \\ \vdots & \vdots & \vdots \\ I_{P_2} & \cdots & I_{P_2} \end{bmatrix}\begin{bmatrix} I_{P_1} \\ \vdots \\ I_{P_1} \end{bmatrix} \tag{17}$$

Claim 2: The subspace spanned by the columns of $\Psi^{P_1}(\Psi^{P_1})^T\Psi^{P_2}$ and the subspace spanned by the columns of $\Psi^{P_2}(\Psi^{P_2})^T\Psi^{P_1}$ is the same, and it is the intersection of the range of Ψ^{P_1} with the range of Ψ^{P_2}.

Proof: The claim is proved in two steps.

1) First, assume P_1 and P_2 are relatively prime. If P_1 and P_2 are relatively prime, the intersection of the two subspaces is the dc subspace. Claims (1), (16), and (17) imply that $\Psi^{P_1}(\Psi^{P_1})^T\Psi^{P_2} = K_0/(P_1P_2) \times \text{ones}(K_0, M_2)$ and $\Psi^{P_2}(\Psi^{P_2})^T\Psi^{P_1} = K_0/(P_1P_2) \times \text{ones}(K_0, M_1)$. Hence, the range of each of the two matrices spans the dc subspace.

2) If P_1 and P_2 are not relatively prime, then let P_3 be the greatest common divisor of P_1 and P_2. The intersection of Ψ^{P_1} and Ψ^{P_2} is then spanned by the range of

$$\begin{bmatrix} I_{P_3} \\ I_{P_3} \\ \vdots \\ I_{P_3} \end{bmatrix}_{K_0 \times P_3}.$$

Rewriting I_{P_1} and I_{P_2} as a function of I_{P_3} gives

$$I_{P_1} = \begin{bmatrix} I_{P_3} & \cdots & 0 \\ \vdots & \ddots & \vdots \\ 0 & \cdots & I_{P_3} \end{bmatrix}_{P_1 \times P_1}$$

and

$$I_{P_2} = \begin{bmatrix} I_{P_3} & \cdots & 0 \\ \vdots & \ddots & \vdots \\ 0 & \cdots & I_{P_3} \end{bmatrix}_{P_2 \times P_2}$$

so that if each I_{P_3} is considered "a unit," then I_{P_1} is a "unit" identity matrix of dimensions $P_1/P_3 \times P_1/P_3$, and I_{P_2} is a "unit" identity matrix of dimensions $P_2/P_3 \times P_2/P_3$. Next, P_2/P_3 and P_1/P_3 are relatively prime. From case (1), this means that

$$\Psi^{P_1}\left(\Psi^{P_1}\right)^T \Psi^{P_2} = \frac{\frac{K_0}{P_3}}{\frac{P_1}{P_3} \times \frac{P_2}{P_3}} \begin{bmatrix} I_{P_3} & \cdots & I_{P_3} \\ \vdots & \ddots & \vdots \\ I_{P_3} & \cdots & I_{P_3} \end{bmatrix}_{K_0 \times M_2} \tag{18}$$

and

$$\Psi^{P_2}\left(\Psi^{P_2}\right)^T \Psi^{P_1} = \frac{\frac{K_0}{P_3}}{\frac{P_1}{P_3} \times \frac{P_2}{P_3}} \begin{bmatrix} I_{P_3} & \cdots & I_{P_3} \\ \vdots & \ddots & \vdots \\ I_{P_3} & \cdots & I_{P_3} \end{bmatrix}_{K_0 \times M_1} \tag{19}$$

The two matrices from (18) and (19) have the same range, and it is the intersection subspace of Ψ^{P_1} with Ψ^{P_2}. ■

ACKNOWLEDGMENT

The authors would like to thank S. Bose, at Schlumberger-Doll Research Center, for his valuable discussions and suggestions on the period estimation problem.

REFERENCES

[1] M. D. Ladd and G. R. Wilson, "Proportional bandwidth properties of fault indicating tones in a ball bearing system," in *Conf. Rec. Twenty-Eighth Asilomar Conf. Signals, Syst., Comput.*, 1995, p. 45.

[2] I. A. Howard, "A review of rolling element bearing vibration detection, diagnosis, and prognosis," Defense Sci. Technol. Org., Canberra, Australia, Tech. Rep. 0013, 1994.

[3] B. Santhanam and P. Maragos, "Harmonic analysis and restoration of separation methods for periodic signal mixtures: Algebraic separation vs comb filtering," *Signal Process.*, vol. 69, no. 1, pp. 81–91, 1998.

[4] M.-Y. Zou, C. Zhenming, and R. Unbehauen, "Separation of periodic signals by using an algebraic method," in *Proc. ISCAS*, vol. 5, 1991, pp. 2427–2430.

[5] M.-Y. Zou and R. Unbehauen, "An algebraic theory for separation of periodic signals," *Archiv fur Elektronik und Uebertragungstechnik*, vol. 45, pp. 351–358, 1991.

[6] A. de Cheveigne, "Separation of concurrent harmonic sounds: Fundamental frequency estimation and a time domain cancellation model of auditory processing," *J. Acoust. Soc. Amer.*, vol. 93, no. 8, pp. 3271–3290, 1993.

[7] L. L. Scharf and B. Friedlander, "Matched subspace detectors," *IEEE Trans. Signal Processing*, vol. 42, pp. 2146–2156, Aug. 1994.

[8] W. A. Sethares and T. W. Staley, "Periodicity transforms," *IEEE Trans. Signal Processing*, pp. 2953–2964, Nov. 1999.

[9] R. T. Behrens and L. L. Scharf, "Signal processing applications of oblique projection operators," *IEEE Trans. Signal Processing*, pp. 1413–1424, May 1994.

[10] L. L. Scharf, *Statistical Signal Processing (Detection, Estimation, and Time Series Analysis)*. Reading, MA: Addison-Wesley, 1991.

[11] S. M. Kay, *Fundamentals of Statistical Signal Processing, Estimation Theory*. Englewood Cliffs, NJ: Prentice-Hall, 1993, vol. 1.

[12] J. D. Wise, J. R. Caprio, and T. W. Parks, "Maximum likelihood pitch estimation," *IEEE Trans. Acoust., Speech, Signal Processing*, vol. 24, pp. 418–421, May 1976.

[13] D. D. Muresan and T. W. Parks, "Orthogonal subspace decomposition of periodic signals," in *Conf. Rec. Thirty-Third Asilomar Conf. Signals, Syst., Comput.*, vol. 2, 1999, pp. 1087–1091.

[14] ——, "A new approach to period estimation," in *Proc. IEEE Int. Conf. Acoust., Speech, Signal Processing*, vol. 2, 2000, pp. 709–712.

[15] (2002). DSP Lab., Cornell Univ., Ithaca, NY. [Online]. Available: http://dsplab.ece.cornell.edu

[16] W. A. Sethares and T. W. Staley. (1999). [Online]. Available: http://ece-serv0.ece.wisc.edu/~sethares

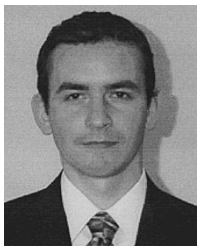

D. Darian Muresan received the B.S. degree in mathematics and electrical engineering from University of Washington, Seattle, and the M.Eng. and Ph.D. degrees in electrical and computer engineering from Cornell University, Ithaca, NY.

His interests include image and signal processing and hardware design. He is the co-inventor of an analog-to-digital converter and has several other patents pending. He interned with HP as a Hardware Design Engineer and is the founder of Digital Multi-Media Design, Arlington, VA (http://www.dmmd.net).

Thomas W. Parks (F'82) received the B.E.E., M.S., Ph.D. degrees from Cornell Unversity, Ithaca, NY.

From 1967 to 1986, he was on the Electrical Engineering faculty at Rice University, Houston, TX. In 1986, he joined Cornell as a Professor of electrical engineering. He has coauthored a number of books on digital signal processing. His research interests are signal theory and digital signal processing.

Dr. Parks received the IEEE Third Millennium Medal and the Humboldt Foundation Senior Scientist Award. He has been a Senior Fulbright Fellow.